Inorganic Chemistry
Cite This: Inorg. Chem. XXXX, XXX, XXX−XXX
Article
pubs.acs.org/IC

A Cancer Cell-Selective and Low-Toxic Bifunctional Heterodinuclear Pt(IV)−Ru(II) Anticancer Prodrug

Lili Ma,[†,§] Xudong Lin,[‡] Cai Li,[†,§] Zoufeng Xu,[†,§] Chun-Yin Chan,[†] Man-Kit Tse,[†] Peng Shi,[‡] and Guangyu Zhu*[,†,§]

[†]Department of Chemistry, City University of Hong Kong, 83 Tat Chee Ave, Hong Kong SAR, People's Republic of China
[‡]Department of Biomedical Engineering, City University of Hong Kong, 83 Tat Chee Ave, Hong Kong SAR, People's Republic of China
[§]City University of Hong Kong Shenzhen Research Institute, Shenzhen 518057, People's Republic of China

Supporting Information

ABSTRACT: Although different types of metal-based anticancer complexes have been synthesized, novel complexes to reduce the serious side effect of cisplatin and conquer cancer metastasis are still highly desired. Here, we report the synthesis, characterization, and biological activity of a novel heterodinuclear Pt(IV)−Ru(II) anticancer prodrug. The Pt(IV)−Ru(II) complex exhibits good stability in both water and PBS solution. Biological evaluation revealed that this bifunctional Pt(IV)−Ru(II) complex utilizes the advantages of two metal centers to have both cytotoxicity and antimetastatic property as designed. Although the complex has comparable cytotoxicities to cisplatin in tested cancer cell lines, this prodrug selectively kills cancer but not normal cells, and the IC_{50} values of the Pt(IV)−Ru(II) complex are 7−10 times higher than those of cisplatin toward normal cells. The cancer cell selectivity is further demonstrated by a cancer−normal cell coculture system. In addition, the antimetastatic properties of the heterodinuclear complex are assessed by using highly metastatic human breast cancer cells, and the results show that the migration and invasion of cancer cells are effectively restrained after the treatment. Moreover, the Pt(IV)−Ru(II) complex displays lower toxicity than cisplatin in developing zebrafish embryos. We, therefore, report an example of heterodinuclear Pt(IV)−Ru(II) complex not only to defeat both drug resistance and cancer metastasis but also having significantly improved cancer cell selectivity and reduced *in vivo* toxicity than cisplatin.

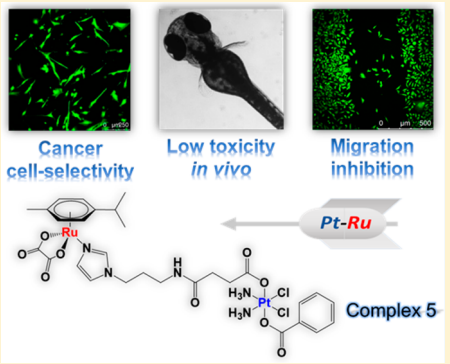

INTRODUCTION

Pt(II)-based anticancer agents including cisplatin and its analogues are among the most widely used and efficient small-molecule drugs in clinical cancer chemotherapy.[1] The serious side effects and the incidence of drug resistance promote the exploitation of new types of metal-based anticancer drug candidates.[2] Pt(IV) complexes represent a promising family of nonconventional Pt-based anticancer agents due to their inertness under physiological conditions, easy modification through axial ligands, and the ability to be activated to Pt(II) by reducing agents after entering cancer cells.[3−5] In the meantime, efforts have been devoted to searching for novel pharmaceutical agents bearing other metals.[6] For example, different from cytotoxic Pt complexes, Ru anticancer drug candidates including NAMI-A and RAPTA-C are well-known for their impressive antimetastatic properties with commonly moderate or low cytotoxicity.[7,8]

It is suggested that the incorporation of different metals into one molecule may induce additive or even synergistic effects. The toxicity of the resulted heteronuclear metal complexes, however, is a great concern due to the presence of different types of metals, and the cancer-cell selectivity of heteronuclear complexes is sometimes overlooked. Indeed, even for mononuclear metal complexes in clinical settings, the dose-related toxicity is usually the cause for therapy discontinuation.[9−11] On the other hand, although some heteronuclear complexes containing Pt have been reported, most work mainly focused on the study of metal−DNA interactions and/or the ability to overcome cisplatin resistance.[12−20] Only few *cis*/*trans*Pt(II)−Ru(III) complexes were reported to be able to effectively combat cancer cell motility.[19] Novel heterodinuclear Pt−Ru complexes with high cytotoxicity and antimetastatic properties against cancer cells but with improved cancer cell-selectivity and low toxicity have been rarely reported and are highly desired.

Herein, we report the synthesis, characterization, and biological evaluation of complex **5**, a heterodinuclear Pt(IV)−Ru(II) complex bearing both cisplatin and arene−Ru(II) moieties. The Pt(IV) unit has advantages over its Pt(II) congener, including but not limited to the kinetic inertness to avoid undesirable side reactions to biomolecules and the

Received: January 7, 2018

DOI: 10.1021/acs.inorgchem.8b00053
Inorg. Chem. XXXX, XXX, XXX−XXX

Scheme 1. (A) Synthetic Route of Complex 5[a] and (B) Synthetic Route of Arene-Ru(II) Compound 6[b]

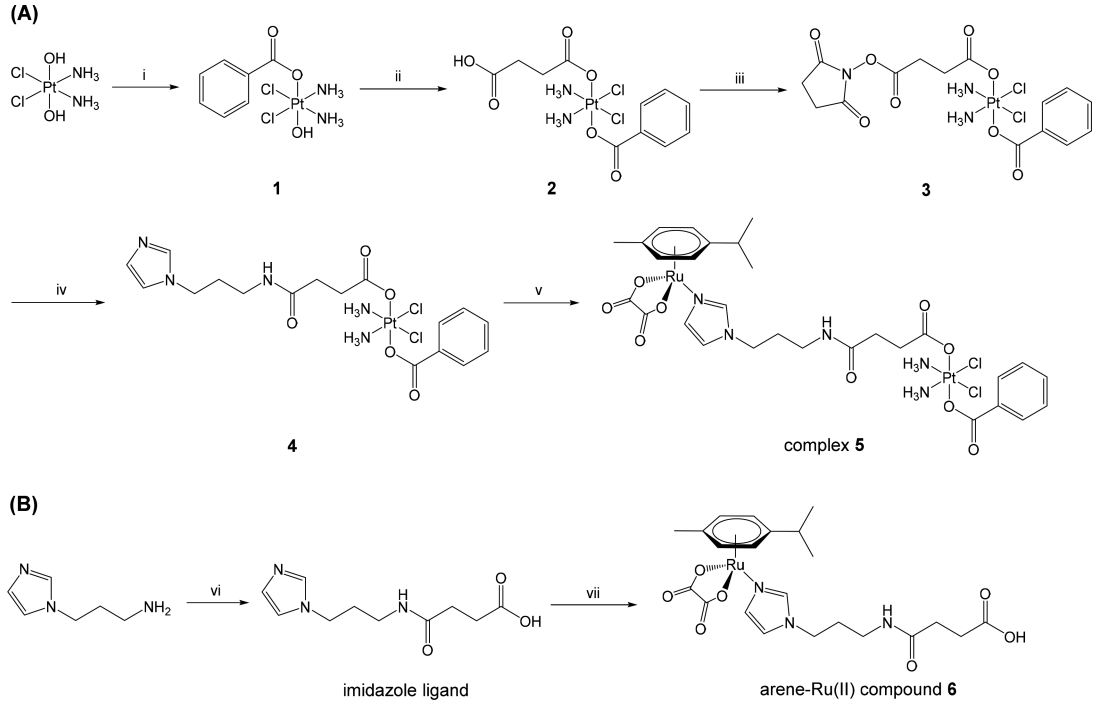

[a]Reagents and conditions: (i) benzoic anhydride, 60 °C, 12 h in DMF; (ii) succinic anhydride, 60 °C, 12 h in DMF; (iii) EDCI/NHS, r.t., 12 h in acetone; (iv) *N*-(3-aminopropyl)-imidazole, r.t., 12 h in acetone; (v) CymRu(II)(O^O)H_2O, r.t., 12 h in methanol. [b]Reagents and conditions: (vi) succinic anhydride, r.t., 12 h in DMF; (vii) CymRu(II)(O^O)H_2O, r.t., 4 h in DCM.

Table 1. Cytotoxicities of Complex 5 and Control Compounds by MTT Assay after 72 h Treatment. IC_{50} Values Are Expressed As the Concentrations of Pt (μM)

cell lines	type	cisplatin	compound **6**	cisplatin + compound **6**[b]	complex **5**
A2780	cancer	1.5 ± 0.3	299 ± 96	1.4 ± 0.2	2.1 ± 0.1
A2780cisR	cancer	9.7 ± 1.0	447 ± 185	7.8 ± 2.3	6.9 ± 4.0
RF[a]		6.5	1.5	5.6	3.2
A549	cancer	3.3 ± 2.5	577 ± 78	1.7 ± 0.5	7.1 ± 3.0
MDA-MB-231	cancer	14 ± 1			30 ± 9
MRC-5	normal	2.9 ± 0.5	>100	1.6 ± 0.3	18 ± 2
WI38	normal	3.2 ± 0.8			24 ± 7
Hs27	normal	12 ± 1			>60
NIH3T3*	normal	4.4 ± 2.0			46 ± 16
SI[c]	normal	0.88		0.98	2.5

[a]RF (resistant factor): IC_{50} in A2780cisR/IC_{50} in A2780. [b]A mixture of cisplatin and an equal equivalent of arene−Ru(II) compound **6**. [c]SI (selectivity index) is defined as IC_{50} in MRC-5/IC_{50} in A549. *Mouse source.

preferred reduction inside cancer cells. To obtain such a bifunctional heterodinuclear anticancer agent, a cytotoxic Pt(IV) unit is conjugated with an arene−Ru(II) center through an imidazole linker. The contribution of Pt to cytotoxicity and Ru to antimetastatic property was illustrated, and the cancer cell-selectivity was scrutinized. The possible relationship between cancer cell selectivity and cellular accumulation was examined. Furthermore, zebrafish embryos were utilized to test the *in vivo* toxicity of complex **5**. We report a unique example of a heterodinuclear Pt(IV)−Ru(II) complex combining the cytotoxic and antimetastatic properties of both metal centers with impressive cancer cell selectivity *in vitro* and low toxicity *in vivo*.

RESULTS AND DISCUSSION

Complex **5** was derived from the asymmetric substitution of *c,c,t*-[$Pt(NH_3)_2Cl_2(OH)_2$] stepwise (Scheme 1). First, the reaction of *c,c,t*-[$Pt(NH_3)_2Cl_2(OH)_2$] with two equivalents of benzoic anhydride yielded *c,c,t*-[$Pt(NH_3)_2Cl_2(OH)$(benzoate)] (**1**). Compound **2** was obtained by the reaction of compound **1** with 6 equiv of succinic anhydride. The carboxylic group of **2** was activated by EDC/NHS chemistry to obtain an NHS ester, followed by conjugation with *N*-(3-aminopropyl)-imidazole through an amide bond to form compound **4**. Finally, the arene−Ru(II) moiety with an oxalate leaving group was applied to **4** to produce the final product **5**.[21,22] Additionally, the arene−Ru(II) compound **6** was synthesized as a control (Scheme 1). The compounds were fully characterized by ^1H, ^{13}C, ^{195}Pt NMR spectroscopy, ESI-MS, and CHN elemental analysis (Figures S1−S16). The purities of compounds **4** and **5**

DOI: 10.1021/acs.inorgchem.8b00053
Inorg. Chem. XXXX, XXX, XXX−XXX

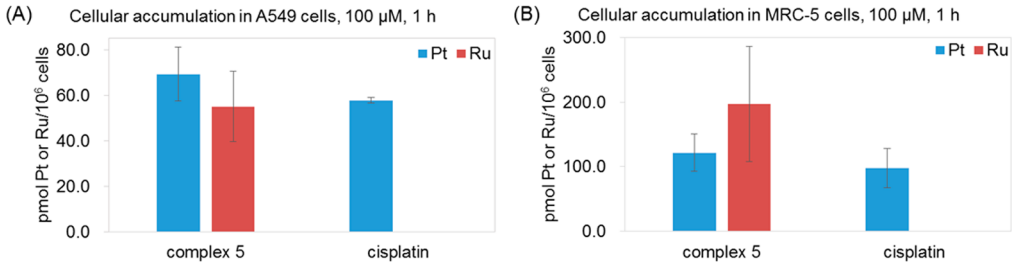

Figure 1. Cellular accumulation of complex **5** and cisplatin in (A) A549 and (B) MRC-5. Cells were treated with 100 μM compounds for 1 h. Cell numbers were recorded, and the Pt or Ru levels were determined by ICP-MS. Data were obtained from two independent experiments and expressed as pmol Pt or Ru per 10^6 cells.

were further tested by HPLC (Figure S17), which are 95% and 96%, respectively.

The stability of the heterodinuclear complex **5** in water was studied by ^{1}H NMR. Mononuclear Pt(IV) compound **4** was included as a control. No significant changes are observed in the spectra of both compounds **4** and **5** after 24 h, indicating their stability in water and excluding the possibility of the ester bond hydrolysis in the Pt(IV) center (Figures S18 and S19).[23] Subsequently, the stability test was carried out in PBS (pH = 7.4). Neither compound **4** nor **5** changes significantly after 24 h under this condition (Figures S20 and S21). The great stability of the compounds will benefit their further biological applications.

Cytotoxicities of complex **5** were evaluated by MTT assay in a panel of human cancer cell lines including A2780 ovarian, A549 non-small-cell lung, and MDA-MB-231 breast cancer cells, which are widely used for the assessment of metal-based anticancer drugs.[24,25] Cisplatin-resistant A2780cisR cells, generated from their parental cells, were also employed.[26] Cisplatin, arene−Ru(II) compound **6**, and a mixture of cisplatin and an equal equivalent of compound **6** were tested as controls. The results are summarized in Table 1. Cisplatin shows cytotoxicity in both cancer and normal cells, and the IC_{50} values were in the low micromolar range. As expected, the cytotoxicity of arene−Ru(II) compound **6** is low, indicated by the high IC_{50} values (>100 μM). In addition, we examined the cytotoxicity of a mixture of cisplatin and an equal equivalent of compound **6**. The mixture shows slightly improved cytotoxicities than cisplatin in the tested cancer cells, including A2780, A2780cisR, and A549 cells. Moreover, in A549 cells, the combination index (CI) tested by Chou-Talalay assay was 0.54, indicating a synergistic effect for the cotreatment of cisplatin and compound **6**. However, the mixture also exhibits a higher cytotoxicity than cisplatin in MRC-5 human normal lung fibroblasts. Cotreatment of cisplatin and compound **6** results in enhanced cytotoxicity but not cancer cell selectivity. We subsequently examined the cytotoxicity of heterodinuclear complex **5**. Complex **5** displays low micromolar IC_{50} values in the tested cancer cells, which are slightly higher than or identical to those of cisplatin and a mixture of cisplatin and compound **6**. For example, the IC_{50} values of cisplatin and the mixture are 1.5 μM and 1.4 μM in A2780 cells, respectively, and that of complex **5** is 2.1 μM. In cisplatin-resistant A2780cisR cells, complex **5** shows a lower IC_{50} value (6.9 μM) than cisplatin (9.7 μM) as well as the mixture (7.8 μM), indicating the effectiveness of complex **5** in the resistant cells. The IC_{50} values of complex **5** are 7.1 and 30 μM in A549 and MDA-MB-231 cells, respectively.

Serious side effects of cisplatin, a metal-based DNA damaging agent without cancer cell selectivity, are always a concern in clinical chemotherapy. The effect of complex **5** on the proliferation of normal cells was subsequently tested. WI38 and MRC-5 normal human lung fibroblast, Hs27 human foreskin fibroblast, and NIH3T3 mouse musculus fibroblast cells were selected for the evaluation (Table 1). Intriguingly, complex **5** shows dramatically decreased cytotoxicities in all the normal cells tested. The IC_{50} values of complex **5** are 7- to 10-fold higher than those of cisplatin in WI38, MRC-5, and NIH3T3 cells. Compared to a mixture of cisplatin and compound **6**, the heterodinuclear complex **5** shows 11-times increased IC_{50} values in MRC-5 cells. In addition, upon treatment with 60 μM of complex **5** for 72 h, the viability of Hs27 cells does not change significantly (Figure S22). The selectivity index (SI), defined as the ratio of the IC_{50} value in MRC-5 to that in A549 cells, is 2.5 for complex **5** but only 0.88 and 0.98 for cisplatin and the mixture, respectively. Taken together, complex **5** shows identical cytotoxicities to those of cisplatin or a mixture of cisplatin and compound **6** in difference types of human cancer cells, but its cytotoxicities are much lower than both in tested normal cells, indicating the significantly improved cancer cell selectivity. The cancer cell selectivity of complex **5** was further demonstrated by coculture of MRC-5 and A549 cells, both of which are originated from the lung and can be easily distinguished by their shapes. Compared to the untreated or cisplatin-treated groups, upon treatment with 50 μM complex **5** for 48 h, very few cancer cells were left, and the normal cells were still alive (Figure S23). The result confirms that the heterodinuclear complex **5** is able to kill cancer cells effectively and selectively.[27]

To probe whether the origin of cancer cell selectivity of complex **5** was from the difference in cellular accumulation, A549 and MRC-5 cells were treated with 100 μM complex **5** or cisplatin for 1 h, and the cellular levels of Pt and Ru were determined by ICP-MS (Figure 1). In A549 and MRC-5 cells, the accumulation levels of complex **5** are identical to those of cisplatin (expressed as Pt levels). For instance, in A549 cells, the cellular level of complex **5** is 69.2 pmol Pt/10^6 cells, and the value for cisplatin is 57.8 pmol Pt/10^6 cells. Similarly, in MRC-5 cells, the cellular uptake of complex **5** and cisplatin are 121.5 pmol Pt/10^6 cells and 97.6 pmol Pt/10^6 cells, respectively. It is noteworthy that both complex **5** and cisplatin show stronger abilities to internalize into MRC-5 cells than A549 cells. Therefore, cellular accumulation may not contribute to the cancer cell-selectivity of complex **5**.

Unlike cisplatin and other types of cytotoxic Pt compounds, the antimetastatic property of Ru complexes is commonly more attractive than their cytotoxicity. Both Ru(III) (e.g., NAMI-A)

DOI: 10.1021/acs.inorgchem.8b00053
Inorg. Chem. XXXX, XXX, XXX−XXX

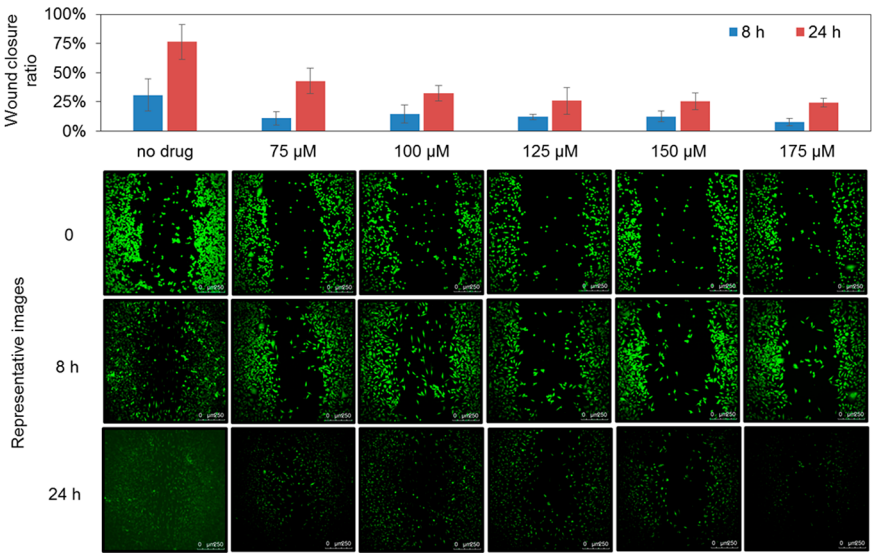

Figure 2. Migration inhibition of MDA-MB-231 cells by wound healing assay. Cells were treated with different concentrations of complex **5**. After calcein-AM staining, images were taken at 0, 8, and 24 h by SPE confocal (10×). Scale bar, 250 μm. The area of the wounds was measured by the ImageJ software. The wound closure ratios were calculated from three to four replicates.

and Ru(II) complexes (e.g., RAPTA-C) have shown their ability to actively suppress cancer metastasis, which is a complicated process from a series of actions.[28−30] To investigate whether the incorporation of arene−Ru(II) moiety into complex **5** is able to functionalize the heterodinuclear complex with antimetastatic ability, we investigated two important steps of metastasis, namely cancer cell migration and invasion.[31] The ability of complex **5** to modulate cancer cell metastasis was measured by using highly metastatic MDA-MB-231 human breast cancer cells. First, the migration inhibition effect of complex **5** was assessed by a wound healing assay (Figure 2).[32] After the formation of a cell monolayer, "wounds" with similar sizes were created, and the initial areas were recorded. Data are listed in Table S1. Subtoxic concentrations of complex **5** were used to minimize its cell-killing effect, and the cell viability was above 75% at 175 μM (Figure S24). In the untreated group, 31% of the scratched area is filled with cells after 8 h. In the treated groups, wound closure ratios range from 15% to 8% with increasing concentrations of complex **5** (from 75 μM to 175 μM), indicating that cell migration is effectively diminished by the complex. A similar trend is observed after 24 h. A total of 76% of the wounds are healed in the untreated group. In contrast, the wound closure ratio is only 25% for the cells treated with 175 μM complex **5**. Even at the lowest concentration used, the wound closure ratio is 43%, which is much lower than the group without treatment. These results show that the heterodinuclear Pt(IV)−Ru(II) complex is able to restrain cancer cell migration in a time- and concentration-dependent manner.

Next, the potential of complex **5** to overcome cancer cell invasion was tested by using a transwell invasion assay.[32,33] The microporous insert wells were precoated with a proper concentration of matrigel to mimic the extracellular matrix. A DMEM medium with 10% FBS was added to the receiver wells as a chemoattractant (Figure S25). MDA-MB-231 cells were treated with 100 μM complex **5** for 24 h, and the cells without treatment were set as a control. After invading to the lower side of the inset wells, cells were stained with crystal violet, and the invasion values were calculated by measuring the UV absorbance at 590 nm. Representative images are shown in Figure 3. As expected, a large number of cells in the control group invades to the lower side of the insets, and the invasion

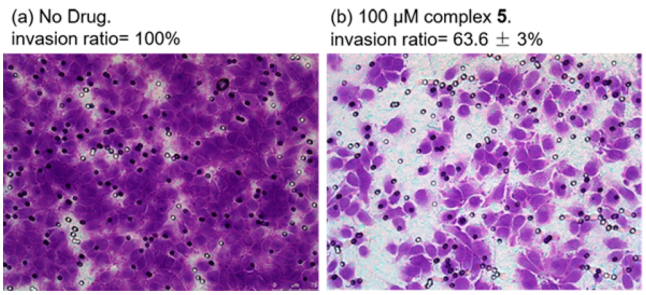

Figure 3. A transwell invasion assay showing the invasion inhibition of MDA-MB-231 by complex **5**. Cells were treated with 100 μM complex **5** for 24 h. Images were taken by a Leica DMI3000 B inverted microscope (20×). Scale bar, 75 μm. Cell invasion ratios were measured by crystal violet assay. The invasion ratio of cells without drug treatment was set as 100%. Data were calculated from two to three replicates.

ratio is defined as 100%. Notably, with the treatment of complex **5**, the invasion ratio reduces to 63.6%. These results demonstrate that complex **5** is able to efficiently inhibit the migration and halt the invasion of MDA-MB-231 cells.

Finally, the *in vivo* toxicity assessment of cisplatin and complex **5** was conducted using zebrafish embryos.[34] With the high degree of homology to mammals, rapid postfertilization development, small size, and optical transparency, zebrafish embryos have become a widely used model organism for drug discovery and toxicology evaluation.[35,36] The embryos were treated with increasing concentrations of cisplatin or complex **5**. The cumulative survival and hatching status of the embryos were recorded and evaluated every 24 h (Figure 4 and Table S2). The mortality and hatching of the embryos are dependent on the concentration of cisplatin and complex **5**. Without treatment, almost all of the zebrafish embryos survive, and they finally develop into juvenile zebrafish. After 96 h of treatment, only when the concentration of cisplatin is 30 μM or lower, the survival rate can maintain over 90%, and the value drops to 75%

DOI: 10.1021/acs.inorgchem.8b00053
Inorg. Chem. XXXX, XXX, XXX−XXX

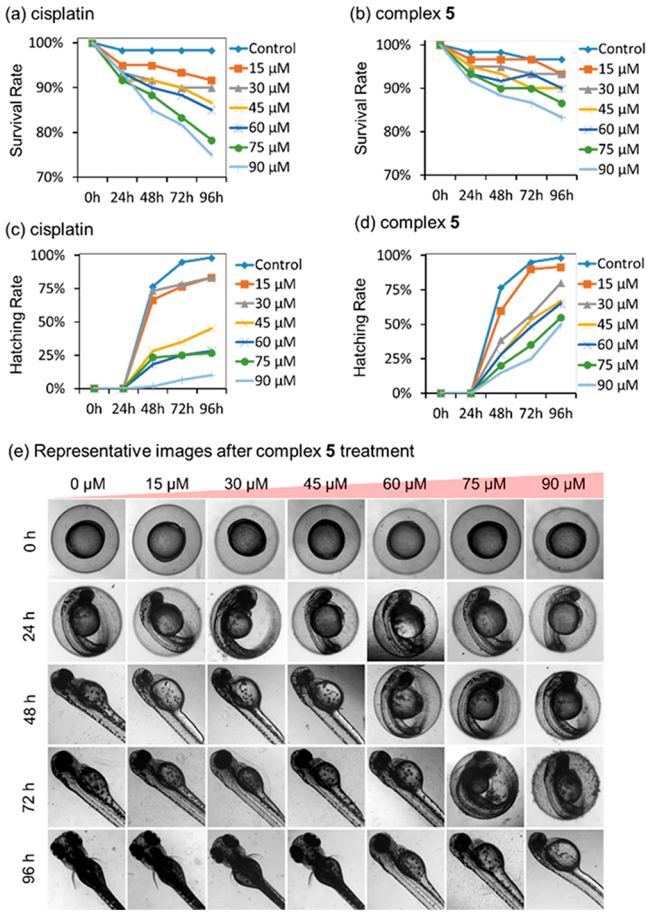

Figure 4. Toxicity assessments of cisplatin and complex **5** using zebrafish embryos. Survival rates of zebrafish embryos in the presence of (a) cisplatin and (b) complex **5** are shown, together with hatching rates of zebrafish embryos after the exposure to (c) cisplatin and (d) complex **5**. (e) Representative ecotoxicology images of zebrafish embryos with treatment of complex **5** at different concentrations over 96 h. Data are collected from four replicates of two independent experiments, and the mean values are presented. The data are also listed in Table S2.

when 90 μM cisplatin is used (Figure 4a). In comparison to cisplatin, the complex-**5**-treated group shows higher survival rates at all the concentrations. The survival rate remains above 90% in the presence of 60 μM complex **5**, and more than 83% of zebrafish embryos survive when the concentration increases to 90 μM (Figure 4b). The hatching rate upon treatment was subsequently measured. In general, the embryos become abnormal and are difficult to develop to juvenile zebrafish with 45 μM or higher concentration of cisplatin. The hatching rate is only 45% upon treatment with 45 μM cisplatin for 96 h. When the concentration increases to 90 μM, only 10% of embryos are able to develop to juvenile zebrafish (Figure 4c). In contrast, the hatching rate upon treatment with even the highest concentration of complex **5** still maintains at 50% after 96 h (Figure 4d), and the representative ecotoxicology images of zebrafish embryos with the treatment of complex **5** are shown in Figure 4e. Collectively, these results suggest that complex **5** has a lower toxicity to zebrafish embryos than cisplatin.

CONCLUSIONS

In conclusion, we report the first example of a heterodinuclear Pt(IV)−Ru(II) complex not only to conquer both drug resistance and cancer metastasis but also having significantly improved cancer cell selectivity and reduced *in vivo* toxicity than cisplatin. The complex utilizes the unique properties of both Pt and Ru metals as designed, and its cytotoxic and antimetastatic properties are confirmed. Although the complex has improved cytotoxicity compared with cisplatin in the resistant cells, its IC_{50} values in several normal cells increase by an order of magnitude, and the complex shows great cancer cell selectivity in a coculture system *in vitro*. The cancer cell selectivity is not due to the cellular accumulation, and we assume that the complex may have selective activation in cancer cells, leading to cancer cell-selectivity. The low toxicity profile of complex **5** is further illustrated by an *in vivo* toxicity assessment using zebrafish embryos. This cancer cell selective and low-toxic bifunctional heterodinuclear compound distinguishes itself from many other types of multinuclear metal-based complexes including the ones made from our own group because their cancer cell selectivity and toxicity are greatly concerned.[10,21] The detailed intracellular fate of complex **5** as well as the profound mechanism of superior cancer cell selectivity are still under investigation.

EXPRIMENTAL SECTION

Materials and Instruments. Cisplatin was purchased from Shandong Boyuan Pharmaceutical Co., Ltd., China. $RuCl_3{\cdot}nH_2O$ was bought from J & K scientific. *N*-[3-(Dimethylamino)propyl]-*N*′-ethylcarbodiimide hydrochloride (EDCI) and succinic anhydride were purchased from Meryer. *N*-Hydroxysuccinimide (NHS) and *N*-(3-aminopropyl)-imidazole were purchased from Sigma-Aldrich. *N*,*N*′-dicyclohexylcarbodiimide (DCC) was ordered from International Laboratory USA. Benzoic anhydride was bought from Energy Chemical. 3-(4,5-Dimethylthiazol-2-yl)-2,5-diphenyltetrazolium bromide (MTT) were purchased from Life Technologies. Transwell insert wells (Corning #3422, 6.5 mm diameter inserts, and 8.0 μm pore size) and Matrigel (Corning #356237) were ordered from Corning. Calcein-AM and crystal violet were purchased from Sigma-Aldrich. All agents and solvents were used as received without additional drying or purification except otherwise indicated. All reactions were carried out under atmosphere unless further notifications. Bruker Ultrashield NMR spectrometers (300, 400, or 600 MHz) were used to detect ^{1}H, ^{13}C, and ^{195}Pt NMR spectra at room temperature. All NMR chemical shifts (δ) are reported in parts per million (ppm) and referenced as described below. ^{1}H and ^{13}C NMR spectra were referenced internally to residual solvent peaks (DMSO-d_6: ^{1}H, δ 2.50; ^{13}C, δ 39.5; D_2O: ^{1}H, δ 4.71). The ^{195}Pt NMR spectrum was referenced externally using standards of K_2PtCl_4 in D_2O (δ = −1628 ppm). Stability tests were carried out by ^{1}H NMR with water suppression, and D_2O was used as an external standard. ESI-MS was carried out on an Agilent API-2000 mass spectrometer (methanol as solvent). Elemental analysis was performed by using a Vario Micro elemental analyzer. Analytical reversed-phase HPLC was carried out by using a Shimadzu Prominence System equipped with a DGU-$20A_{SR}$ Degasser, two LC-20AT Liquid Chromatography Pumps, a SPD-20A UV/vis detector, and a C18 column (Phenomenex, Gemini, 5 μm, 110 Å, 250 × 4.6 mm). An inductively coupled plasma-optical emission spectrometer (ICP-OES, Optima 2100DV, PerkinElmer, USA) or inductively coupled plasma-mass spectrometer (ICP-MS, NEXION 2000, PerkinElmer, USA) was applied to determine platinum and ruthenium levels. Confocal images of the coculture assay and wound healing assay were taken by a Leica SPE confocal microscope. Photos of the transwell invasion assay were taken with a Leica DMI3000 B inverted microscope. Images for *in vivo* toxicity test by zebrafish

DOI: 10.1021/acs.inorgchem.8b00053
Inorg. Chem. XXXX, XXX, XXX−XXX

embryo were taken with an inverted microscope (Olympus IX81) equipped with a cooled sCMOS camera (Neo, ANDOR).

HPLC Analysis of Compounds Purity. Phase A: milli-Q H_2O with 0.02% TFA. Phase B: acetonitrile (ACN) with 0.02% TFA. Program: 0−12 min, 80% to 30% phase A; 12−14 min, 30% phase A; 14−15 min, 30% to 80% phase A; 16 min, stop. Flow rate: 1.0 mL/min. Injection volume: 20 μL, @ 254 and 365 nm. For analysis of compounds' purity, a certain amount of compound **4** or **5** was dissolved in Milli-Q-H_2O and injected for a purity test. The integral was calculated according to absorbance at 254 nm.

Stability Test by ^{1}H NMR. The powder of compound **4** or **5** was dissolved in Milli-Q-H_2O or PBS with 1.6 or 2 mM as the final concentration just before the test. ^{1}H NMR spectra were acquired on a Bruker Ultrashield 600 MHz NMR spectrometer with water suppression.

Synthesis of Compound 1. The *c,c,t*-$[Pt(NH_3)_2Cl_2(OH)_2]$ (200.0 mg, 0.60 mmol, 1.0 equiv) and benzoic anhydride (270.0 mg, 1.20 mmol, 2.0 equiv) were heated to 60 °C in 2 mL of DMF for 16 h in the dark. The suspension changed from yellow into white gradually. Then, the product was collected by centrifugation and washed by acetone and diethyl ether. White powder, 215.0 mg, 82.1%. ^{1}H NMR (300 MHz, DMSO-d_6): δ 7.93−7.84 (m, 2H), 7.58−7.31 (m, 3H), 6.47−5.70 (m, 6H), 1.15 (t, *J* = 11.4 H, 1H). ^{13}C NMR (100 MHz, DMSO-d_6): δ 173.5, 134.8, 131.1, 129.3, 127.7.

Synthesis of Compound 2. Compound **1** (50.0 mg, 0.11 mmol, 1.0 equiv) and succinic anhydride (70.0 mg, 0.70 mmol, 6.1 equiv) were stirred in 1 mL of DMF at 60 °C overnight. The suspension changed into a yellow solution gradually. A large amount of diethyl ether was added to get a white precipitate. The product was washed with diethyl ether. Light yellow powder, 20.0 mg, 33.8%. ^{1}H NMR (400 MHz, DMSO-d_6): δ 12.11 (s, 1H), 7.88 (d, *J* = 7.6 Hz, 2H), 7.52 (t, *J* = 7.2 Hz, 1H), 7.43 (t, *J* = 7.6 Hz, 2H), 7.06−6.17 (m, 6H), 2.54 (t, *J* = 7.2 Hz, 2H), 2.40 (t, *J* = 7.2 Hz, 2H). ^{13}C NMR (100 MHz, DMSO-d_6): δ 179.6, 173.8, 173.3, 133.1, 131.6, 129.4, 127.9, 30.4, 29.8.

Synthesis of Compound 3. Compound **2** (160.0 mg, 0.30 mmol, 1.0 equiv), *N*-hydroxysuccinimide (NHS, 48.0 mg, 0.42 mmol, 1.4 equiv), and DCC (67.5 mg, 1.1 equiv) were stirred in 5 mL of acetone at room temperature for 12 h in the dark. The suspension changed into a yellow solution with white precipitate dicyclohexylurea (DCU). The byproduct DCU was removed by filtration, and the yellow solution was concentrated by rotary evaporation. Yellow powder, 180.2 mg, 94.5%. ^{1}H NMR (400 MHz, DMSO-d_6): δ 7.89 (d, *J* = 8.0 Hz, 2H), 7.53 (t, *J* = 7.3 Hz, 1H), 7.43 (t, *J* = 7.6 Hz, 1H), 7.05−6.27 (m, 6H), 2.88−2.79 (m, 6H), 2.68 (t, *J* = 6.8 Hz, 2H). ^{13}C NMR (100 MHz, DMSO-d_6): δ 178.2, 173.3, 170.2, 168.4, 133.0, 131.7, 129.4, 127.9, 33.4, 30.8, 29.6, 26.7.

Synthesis of Compound 4. Compound **3** (150.0 mg, 0.24 mmol, 1.0 equiv) was dissolved in 5 mL of acetone. A solution of *N*-(3-aminopropyl)-imidazole (31.0 μL, 0.26 mmol. 1.1 equiv) in acetone was added dropwise to compound **3**. Yellow precipitate formed upon the adding of *N*-(3-aminopropyl)-imidazole. After 12 h, the product was collected by centrifugation and washed with diethyl ether. Light yellow powder, 100.3 mg. 65.8%. ^{1}H NMR (400 MHz, DMSO-d_6): δ 7.92 (t, *J* = 5.2 Hz, 1H), 7.89 (d, *J* = 8.0 Hz, 2H), 7.63 (s, 1H), 7.53 (t, *J* = 7.2 Hz, 1H), 7.43 (t, *J* = 7.6 Hz, 2H), 7.18 (s, 1H), 6.89 (s, 1H), 6.97−6.28 (m, 6H), 3.97 (t, *J* = 6.8 Hz, 2H), 3.06−2.96 (m, 2H), 2.31 (t, *J* = 7.6 Hz, 2H), 1.89−1.75 (m, 2H). ^{13}C NMR (100 MHz, DMSO-d_6): δ 180.5, 173.7, 172.0, 137.8, 133.6, 132.1, 129.8, 128.8, 128.3, 119.8, 44.1, 36.2, 31.9, 31.7, 31.2, 31.2. ^{195}Pt NMR (128 MHz, DMSO-d_6): δ 1202. ESI-MS (negative mod, methanol) $C_{17}H_{25}Cl_2N_5O_5Pt$, $[M - H]^-$, cald (*m*/*z*): 644.1. Found: 644.2.

Synthesis of Complex 5. CymRu(II)(O^O)H_2O was synthesized by following the previous procedure.[22] The solution of compound **4** (20.0 mg, 0.03 mmol, 1.0 equiv) in methanol was added dropwise into a solution of CymRu(II)(O^O)H_2O in methanol (10.1 mg, 0.03 mmol, 1.0 equiv). The mixture was stirred at room temperature in the dark for 12 h. After removing solvent by rotary evaporation, the orange product was washed with diethyl ether several times. Orange powder, 20.0 mg, 68.7%. ^{1}H NMR (300 MHz, DMSO-d_6): δ 7.99−7.91 (m, 2H), 7.92−7.86 (m, 2H), 7.59−7.47 (m, 1H), 7.48−7.34 (m, 3H), 6.93−6.42 (m, 7H), 5.75 (d, *J* = 6.0 Hz, 2H), 5.52 (d, *J* = 6.0 Hz, 2H), 4.04 (t, *J* = 6.9 Hz, 2H), 3.01 (q, *J* = 5.7 Hz, 2H), 2.76−2.64 (m, 1H), 2.51 (d, *J* = 7.2 Hz, 2H), 2.32 (d, *J* = 7.2 Hz, 2H), 2.03 (s, 3H), 1.85 (m, 2H), 1.20 (d, *J* = 6.9 Hz, 6H). ^{13}C NMR (150 MHz, DMSO-d_6): δ 180.7, 173.8, 172.2, 165.3, 140.1, 133.7, 132.1, 129.8, 129.3, 128.3, 121.1, 100.0, 97.3, 83.0, 79.5, 45.3, 40.7, 35.6, 32.0, 30.8, 22.6, 17.8. ^{195}Pt NMR (128 MHz, DMSO-d_6): δ 1205. ESI-MS (negative mode, methanol) $C_{29}H_{38}Cl_2N_5O_9PtRu$, $[M - H]^-$, cald (*m*/*z*): 968.1. Found: 968.3. Anal. Calcd for $C_{29}H_{39}Cl_2N_5O_9PtRu{\cdot}2H_2O$: C, 34.67; H, 4.31; N, 6.97. Found: C, 34.49; H, 4.486; N, 6.87. Pt/Ru ratio is 1:1.03 by ICP-OES, and the data are an average from four independent experiments.

Synthesis of Imidazole Ligand. *N*-(3-Aminopropylaminopropyl)-imidazole (715 μL, 6.0 mmol. 1.2 equiv) and succinic anhydride (500 mg, 5.0 mmol. 1.0 equiv) were stirred in 0.7 mL of DMF for 12 h at room temperature. Then, 50 mL of Et_2O was added to the reaction solution to get a white precipitate. The product was collected by filtration and washed with Et_2O (Scheme 1B). White powder, 1.0 g, 88.8%. ^{1}H NMR (300 MHz, DMSO-d_6): δ 11.93 (s, 1H), 7.92 (t, *J* = 6.0 Hz, 1H), 7.61 (s, 1H), 7.17 (s, 1H), 6.88 (s, 1H), 3.95 (t, *J* = 6.0 Hz, 2H), 3.00 (q, *J* = 6.0 Hz, 2H), 2.44 (t, *J* = 6.0, 2H), 2.31 (t, *J* = 6.0, 2H), 1.89−1.74 (m, 2H).

Synthesis of Arene−Ru(II) Compound 6. Compound **6** was synthesized by adding the DCM solution of imidazole ligand (135 mg, 0.6 mmol, 1.0 equiv) dropwise to the DCM solution of CymRu(II)-(O^O)H_2O (202.0 mg, 0.6 mmol, 1.0 equiv). The mixture was reacted at room temperature for 4 h in the dark. Then, DCM was removed by rotary evaporator. Orange oil, 312.7 mg, 95%. ^{1}H NMR (300 MHz, $CDCl_3$): δ 7.63 (s, 1H), 7.48 (t, *J* = 6.0 Hz, 1H), 6.88 (s, 2H), 5.64 (d, *J* = 6.0 Hz, 2H), 5.42 (d, *J* = 6.0 Hz, 2H), 3.72 (t, *J* = 6.0 Hz, 2H), 3.20−3.08 (m, 2H), 2.819−2.75 (m, 1H), 2.72−2.68 (m, 2H), 2.56−2.45 (m, 2H), 2.13 (s, 3H), 1.90−1.76 (m, 2H), 1.29 (d, *J* = 6.0 Hz, 6H).

Cell Lines and Cell Culture Conditions. A2780 and A2780cisR cells were cultured in RPMI 1640 with 10% FBS and 100 units of penicillin/streptomycin. A549, MDA-MB-231, NIH3T3, and Hs27 cells were cultured in DMEM containing 10% FBS and 100 units of penicillin/streptomycin. WI38 and MRC-5 cells were cultured in MEM with 10% FBS, 1% L-glutamine, 1% nonessential amino acids, and 1% sodium pyruvate. Cisplatin-resistant cells A2780cisR were generated from their parental A2780 cells. Briefly, A2780 cells were cultured in complete medium containing 0.5 μg/mL cisplatin at the beginning for the first screening, and the remaining cells were cultured in complete medium containing 1.0 μg/mL cisplatin for at least 4 weeks until the resistance was obtained.[26] All cells were incubated at 37 °C in 5% CO_2.

Cytotoxicity Test. An MTT assay was used to evaluate the *in vitro* cytotoxicity of the compounds. Cells were seeded in 96-well plates at a density of 1500 to 2500 cells per well until the cell confluency reached about 30%. Then, the medium was replaced by a drug-containing medium. DMF was used as a supporting solvent, and its final concentration was 0.5%. Cells incubated with a medium containing 0.5% DMF were set as controls. After 72 or 24 h of drug treatment, the drug-containing medium was removed by FBS-free medium containing 1 mg/mL MTT (0.2 mL per well). The medium was replaced by DMSO after 2 to 4 h of staining (0.2 mL per well). The absorbance was measured at 570 and 730 nm.

Coculture of MRC-5 and A549 Cells. Long-shape MRC-5 cells (15 000 cells/well) and round-shape A549 cells (15 000 cells/well) were seeded in a 24-well plate and were cultured in MEM with 10% FBS, 1% L-glutamine, 1% nonessential amino acids, and 1% sodium pyruvate. Sixteen hours later, the medium was replaced by a medium containing 50 μM cisplatin or complex **5**. Next, 0.5% DMF was used as a supporting solvent, and cells treated with 0.5% DMF were set as a control. After 48 h of treatment, the drug-containing medium was removed, and cells were washed with PBS three times. Then, cells were stained with calcein-AM and washed with PBS three times. Calcein-AM was prepared to 1 mM stock solution in DMSO and was diluted 2000 times with PBS before use. Images were taken with a laser

DOI: 10.1021/acs.inorgchem.8b00053
Inorg. Chem. XXXX, XXX, XXX−XXX

confocal microscope (Leica SPE) with 10× magnification, and the scale bar is 250 μm. The experiment was repeated with four replicates.

Cellular Accumulation. A549 cells or MRC-5 cells were seeded in a six-well plate, and 100 μM of complex **5** or cisplatin was added when the confluency of cells reached around 80%. Cells were incubated with 100 μM compound in complete medium (DMEM for A549 cell, and MEM for MRC-5 cells) for 1 h. Then, cells were collected by trypsinization, and the cell numbers were recorded. The levels of Pt and Ru were determined by ICP-MS after digestion with concentrated HNO_3 at 65 °C overnight. Next, 0.5% DMF was used as a supporting solvent in this experiment. Data were collected from two independent experiments and expressed as pmol Pt or Ru/10^6 cells.

Migration Inhibition by Wound Healing Assay. MDA-MB-231 cells were suspended in DMEM containing 12% FBS and seeded in 24-well plates with a density of 280 000 cells per well. Cells were allowed to attach and grow to form a confluent monolayer. Each well of the plates was marked with a horizontal line passing through the center of the bottom in advance. Wounds were created perpendicular to the lines by tips, and unattached cells were removed by PBS washing (pH 7.4). After calcein-AM staining, cells were washed with PBS three times. Then, cells were incubated in DMEM with 1% FBS containing different concentrations of complex **5** at 37 °C under 5% CO_2. Then, 1% FBS was used to suppress cell proliferation. DMF was used as a supporting solvent, and the final concentration was 1%. Cells with 1% DMF were set as a control. Images were captured at t = 0, 8, and 24 h at the same position of each well. Photos were taken with a laser confocal microscope (Leica SPE) with 10× magnification. Images were generated by using the LAS AF Lite software, and the scale bar is 250 μm. The area of the wounds was measured by using the ImageJ software based on bright field at each time point. In general, the thresholds were adjusted, and the background was set to black first. Then, the filled cells were highlighted from the images by intensity through setting the filters. Finally, the outlines were drawn manually, and the areas of wounds were measured. Wound closure ratio (%) = [(original wound area − wound area at t)/original wound area] × 100%. Data were calculated from three to four replicates.

Invasion Inhibition by Transwell Invasion Assay. Assay preparation: MDA-MD-231 cells were starved in a serum-free medium for 12−16 h before use. Transwell insert wells (Corning #3422, 6.5 mm diameter inserts, and 8.0 μm pore size) were precoated with Matrigel 200−300 μg/mL and 100 μL/insert. After coating with Matrigel, the inset wells were hydrated with 0.1 mL of serum-free medium for 1 h. After harvesting by trypsinization, cells were washed twice with serum-free medium and suspended in serum-free medium (control group) or serum-free medium containing complex **5**. DMF was used as a supporting solvent, and the final concentration was 0.5%. Cells with 0.5% DMF were set as a control. A 100 μL cell suspension containing 50 000 cells was added to each insert. A total of 600 μL of medium with 10% FBS as chemoattractant was added to the receiver wells. The inserts were placed into the receiver wells gently without making bubbles (Figure S25). Then, cells were incubated at 37 °C under 5% CO_2 for 24 h. After removing the medium, the inset wells were removed and generally washed with PBS twice. Cells on the upside of the insets were removed by cotton swabs and the insets washed with PBS twice. Then, cells on the lower side of the inset wells were fixed with 1.1% (w/v) glutaraldehyde for 15 min at room temperature, followed by PBS washing two times and air-drying. Subsequently, cells were stained with 0.1% crystal violet in 200 mM boric acid solution for 20 min. After staining, cells were washed with PBS twice and air-dried. Photos were taken by a Leica DMI3000 B inverted microscope with 20× magnification, and the scale bar is 75 μm. Finally, the crystal violet was dissolved in 10% acetic acid (600 μL/well, 15 min with gently shaking at r.t.). Cell invasion ratios were calculated according to the absorbance at 590 nm. Data were calculated from two to three replicates.

***In Vivo* Toxicity Test by Using Zebrafish Embryos.** The embryos were obtained by random pairwise mating of wild-type adult zebrafish (*Danio rerio*), which were maintained in aquaria under standard laboratory conditions (at 28 ± 1 °C under a cycle of 14 h light, 10 h dark). After collection, the eggs would be transferred to 9 cm Petri dishes containing 0.1 Hanks' Balanced Salt Solution 30 (0.1 HBSS) at pH 7.46 (egg water) according to standard practices. Zebrafish embryos were incubated in 24-well plates with 1 mL solutions containing different concentrations (0, 15, 30, 45, 60, 75, and 90 μM) of cisplatin or complex **5** in egg water at 28 ± 1 °C. No supporting solvent was used in this experiment.[15] Embryos were used per concentration, and four replicates from two independent experiments were carried out. The hatching and growth of the zebrafish embryos without and with cisplatin and complex **5** were monitored every 24 h with an inverted microscope (Olympus IX81) equipped with a cooled sCMOS camera (Neo, ANDOR). All animal work was carried out with prior approval from the animal ethical committee of City University of Hong Kong and was in accordance with local animal care guidelines.

■ ASSOCIATED CONTENT

Supporting Information

The Supporting Information is available free of charge on the ACS Publications website at DOI: 10.1021/acs.inorgchem.8b00053.

Figures S1−S25, Tables S1 and S2 (PDF)

■ AUTHOR INFORMATION

Corresponding Author

*E-mail: guangzhu@cityu.edu.hk.

ORCID

Peng Shi: 0000-0003-0629-4161

Guangyu Zhu: 0000-0002-4710-7070

Author Contributions

The manuscript was written through contributions of L.M., X.L., and G.Z. All authors have given approval to the final version of the manuscript.

Notes

The authors declare no competing financial interest.

■ ACKNOWLEDGMENTS

We thank the National Natural Science Foundation of China (Grant No. 21371145) and the City University of Hong Kong (Projects 7004656, 9667131, and 9667148) for funding support.

■ REFERENCES

(1) Kelland, L. The resurgence of platinum-based cancer chemotherapy. *Nat. Rev. Cancer* **2007**, *7*, 573−584.

(2) Burger, H.; Loos, W. J.; Eechoute, K.; Verweij, J.; Mathijssen, R. H. J.; Wiemer, E. A. C. Drug transporters of platinum-based anticancer agents and their clinical significance. *Drug Resist. Updates* **2011**, *14*, 22−34.

(3) Johnstone, T. C.; Suntharalingam, K.; Lippard, S. J. The Next Generation of Platinum Drugs: Targeted Pt(II) Agents, Nanoparticle Delivery, and Pt(IV) Prodrugs. *Chem. Rev.* **2016**, *116*, 3436−3486.

(4) Wilson, J. J.; Lippard, S. J. Synthetic methods for the preparation of platinum anticancer complexes. *Chem. Rev.* **2014**, *114*, 4470−4495.

(5) Basu, U.; Banik, B.; Wen, R.; Pathak, R. K.; Dhar, S. The platin-X series: activation, targeting, and delivery. *Dalton Trans.* **2016**, *45*, 12992−13004.

(6) Muhammad, N.; Guo, Z. Metal-based anticancer chemotherapeutic agents. *Curr. Opin. Chem. Biol.* **2014**, *19*, 144−153.

(7) Zhang, P.; Sadler, P. J. Redox-active metal complexes for anticancer therapy. *Eur. J. Inorg. Chem.* **2017**, *2017*, 1541−1548.

(8) Alessio, E. Thirty years of the drug candidate NAMI-A and the myths in the field of ruthenium anticancer compounds: a personal perspective. *Eur. J. Inorg. Chem.* **2017**, *2017*, 1549−1560.

(9) Leijen, S.; Burgers, S. A.; Baas, P.; Pluim, D.; Tibben, M.; van Werkhoven, E.; Alessio, E.; Sava, G.; Beijnen, J. H.; Schellens, J. H. M.

DOI: 10.1021/acs.inorgchem.8b00053
Inorg. Chem. XXXX, XXX, XXX−XXX

Phase I/II study with ruthenium compound NAMI-A and gemcitabine in patients with non-small cell lung cancer after first line therapy. *Invest. New Drugs* **2015**, *33*, 201−214.
(10) Bergamo, A.; Sava, G. Linking the future of anticancer metal-complexes to the therapy of tumour metastases. *Chem. Soc. Rev.* **2015**, *44*, 8818−8835.
(11) Galanski, M.; Jakupec, M. A.; Keppler, B. K. Update of the preclinical situation of anticancer platinum complexes: novel design strategies and innovative analytical approaches. *Curr. Med. Chem.* **2005**, *12*, 2075−2094.
(12) Jovanovic, S.; Obrencevic, K.; Bugarcic, Z. D.; Popovic, I.; Zakula, J.; Petrovic, B. New bimetallic palladium(II) and platinum(II) complexes: studies of the nucleophilic substitution reactions, interactions with CT-DNA, bovine serum albumin and cytotoxic activity. *Dalton Trans.* **2016**, *45*, 12444−12457.
(13) Ramu, V.; Gill, M. R.; Jarman, P. J.; Turton, D.; Thomas, J. A.; Das, A.; Smythe, C. A cytostatic ruthenium(II)−platinum(II) bis(terpyridyl) anticancer complex that blocks entry into Sphase by up-regulating p27KIP1. *Chem. - Eur. J.* **2015**, *21*, 9185−9197.
(14) van der Schilden, K.; Garcìa, F.; Kooijman, H.; Spek, A. L.; Haasnoot, J. G.; Reedijk, J. A highly flexible dinuclear ruthenium(II)−platinum(II) complex: Crystal structure and binding to 9-ethylguanine. *Angew. Chem., Int. Ed.* **2004**, *43*, 5668−5670.
(15) Miao, R.; Mongelli, M. T.; Zigler, D. F.; Winkel, B. S. J.; Brewer, K. J. A multifunctional tetrametallic Ru−Pt supramolecular complex exhibiting both DNA binding and photocleavage. *Inorg. Chem.* **2006**, *45*, 10413−10415.
(16) Prussin, A. J., II; Zhao, S.; Jain, A.; Winkel, B. S. J.; Brewer, K. J. DNA interaction studies of tridentate bridged Ru(II)−Pt(II) mixed-metal supramolecules. *J. Inorg. Biochem.* **2009**, *103*, 427−431.
(17) Higgins, S. L. H.; White, T. A.; Winkel, B. S. J.; Brewer, K. J. Redox, spectroscopic, and photophysical properties of Ru−Pt mixed-metal complexes incorporating 4,7-diphenyl-1,10-phenanthroline as efficient DNA binding and photocleaving agents. *Inorg. Chem.* **2011**, *50*, 463−470.
(18) Jain, A.; Winkel, B. S. J.; Brewer, K. J. In vivo inhibition of E. coli growth by a Ru(II)/Pt(II) supramolecule $[(tpy)RuCl(dpp)PtCl_2](PF_6)$. *J. Inorg. Biochem.* **2007**, *101*, 1525−1528.
(19) Herman, A.; Tanski, J. M.; Tibbetts, M. F.; Anderson, C. M. Synthesis, characterization, and in vitro evaluation of a potentially selective anticancer, mixed-metal [ruthenium(III)−platinum(II)] trinuclear complex. *Inorg. Chem.* **2008**, *47*, 274−280.
(20) Anderson, C. M.; Taylor, I. R.; Tibbetts, M. F.; Philpott, J.; Hu, Y.; Tanski, J. M. Hetero-multinuclear ruthenium(III)/platinum(II) complexes that potentially exhibit both antimetastatic and antineoplastic properties. *Inorg. Chem.* **2012**, *51*, 12917−12924.
(21) Ma, L.; Ma, R.; Wang, Z.; Yiu, S.-M.; Zhu, G. Heterodinuclear Pt(IV)-Ru(II) anticancer prodrugs to combat both drug resistance and tumor metastasis. *Chem. Commun.* **2016**, *52*, 10735−10738.
(22) Ang, W. H.; De Luca, A.; Chapuis-Bernasconi, C.; Juillerat-Jeanneret, L.; Lo Bello, M.; Dyson, P. J. Organometallic ruthenium inhibitors of glutathione-S-transferase P1−1 as anticancer drugs. *ChemMedChem* **2007**, *2*, 1799−1806.
(23) Wexselblatt, E.; Raveendran, R.; Salameh, S.; Friedman-Ezra, A.; Yavin, E.; Gibson, D. On the stability of Pt^{IV} pro-drugs with haloacetato ligands in the axial positions. *Chem. - Eur. J.* **2015**, *21*, 3108−3114.
(24) Wang, Z.; Xu, Z.; Zhu, G. A platinum(IV) anticancer prodrug targeting nucleotide excision repair to overcome cisplatin resistance. *Angew. Chem., Int. Ed.* **2016**, *55*, 15564−15568.
(25) Raveendran, R.; Braude, J. P.; Wexselblatt, E.; Novohradsky, V.; Stuchlikova, O.; Brabec, V.; Gandin, V.; Gibson, D. Pt(IV) derivatives of cisplatin and oxaliplatin with phenylbutyrate axial ligands are potent cytotoxic agents that act by several mechanisms of action. *Chem. Sci.* **2016**, *7*, 2381−2391.
(26) Liang, X.-J.; Meng, H.; Wang, Y.; He, H.; Meng, J.; Lu, J.; Wang, P. C.; Zhao, Y.; Gao, X.; Sun, B.; Chen, C.; Xing, G.; Shen, D.; Gottesman, M. M.; Wu, Y.; Yin, J.-j.; Jia, L. Metallofullerene nanoparticles circumvent tumor resistance to cisplatin by reactivating endocytosis. *Proc. Natl. Acad. Sci. U. S. A.* **2010**, *107*, 7449−7454.
(27) Dhar, S.; Lippard, S. J. Mitaplatin, a potent fusion of cisplatin and the orphan drug dichloroacetate. *Proc. Natl. Acad. Sci. U. S. A.* **2009**, *106*, 22199−22204.
(28) Dyson, P. J.; Sava, G. Metal-based antitumour drugs in the post genomic era. *Dalton Trans.* **2006**, 1929−1933.
(29) Gupta, G. P.; Massagué, J. Cancer metastasis: building a framework. *Cell* **2006**, *127*, 679−695.
(30) Muller, A.; Homey, B.; Soto, H.; Ge, N.; Catron, D.; Buchanan, M. E.; McClanahan, T.; Murphy, E.; Yuan, W.; Wagner, S. N.; Barrera, J. L.; Mohar, A.; Verastegui, E.; Zlotnik, A. Involvement of chemokine receptors in breast cancer metastasis. *Nature* **2001**, *410*, 50−56.
(31) Wan, L.; Pantel, K.; Kang, Y. Tumor metastasis: moving new biological insights into the clinic. *Nat. Med.* **2013**, *19*, 1450−1464.
(32) Valster, A.; Tran, N. L.; Nakada, M.; Berens, M. E.; Chan, A. Y.; Symons, M. Cell migration and invasion assays. *Methods* **2005**, *37*, 208−215.
(33) Albini, A.; Iwamoto, Y.; Kleinman, H. K.; Martin, G. R.; Aaronson, S. A.; Kozlowski, J. M.; McEwan, R. N. A rapid *in vitro* assay for quantitating the invasive potential of tumor cells. *Cancer Res.* **1987**, *47*, 3239−3245.
(34) Zon, L. I.; Peterson, R. T. In vivo drug discovery in the zebrafish. *Nat. Rev. Drug Discovery* **2005**, *4*, 35−44.
(35) Lenis-Rojas, O. A.; Fernandes, A. R.; Roma-Rodrigues, C.; Baptista, P. V.; Marques, F.; Perez-Fernandez, D.; Guerra-Varela, J.; Sanchez, L.; Vazquez-Garcia, D.; Torres, M. L.; Fernandez, A.; Fernandez, J. J. Heteroleptic mononuclear compounds of ruthenium-(II): synthesis, structural analyses, in vitro antitumor activity and in vivo toxicity on zebrafish embryos. *Dalton Trans.* **2016**, *45*, 19127−19140.
(36) Wu, Q.; Zheng, K.; Liao, S.; Ding, Y.; Li, Y.; Mei, W. Arene ruthenium(II) complexes as low-toxicity inhibitor against the proliferation, migration, and invasion of MDA-MB-231 cells through binding and stabilizing c-myc G-quadruplex DNA. *Organometallics* **2016**, *35*, 317−326.

DOI: 10.1021/acs.inorgchem.8b00053
Inorg. Chem. XXXX, XXX, XXX−XXX